

# Green Platinum Nanoparticles Interaction With HEK293 Cells: Cellular Toxicity, Apoptosis, and Genetic Damage

Dose-Response:  
An International Journal  
October-December 2018:1-11  
© The Author(s) 2018  
Article reuse guidelines:  
sagepub.com/journals-permissions  
DOI: 10.1177/1559325818807382  
journals.sagepub.com/home/dos



Rafa S. Almeer<sup>1</sup>, Daoud Ali<sup>1</sup>, Saud Alarifi<sup>1</sup>, Saad Alkahtani<sup>1</sup> , and Mansour Almansour<sup>1</sup>

## Abstract

Metal nanoparticles are widely used in industry, agriculture, textiles, drugs, and so on. The adverse effect of green platinum nanoparticles on human embryonic kidney (HEK293) cells is not well established. In the current study, green platinum nanoparticles were synthesized using leaf extract of *Azadirachta indica* L. Green platinum nanoparticles were characterized by dynamic light scattering and transmission electron microscope. The cytotoxicity of green platinum nanoparticle was observed in HEK293 cells by applying 3-(4,5-dimethylthiazol-2-yl)-5-(3-carboxymethoxyphenyl)-2-(4-sulfophenyl)-2H-tetrazolium (MTS) and Neutral red uptake (NRU) assays. Cell viability of the cells was decreased in a concentration and duration-dependent manner. Generation of reactive oxygen species (ROS) in HEK293 cells due to green platinum nanoparticles was examined using fluorescent dye 2,7-dichlorofluorescein diacetate (DCFDA), and ROS was increased according to exposure pattern. The cytotoxicity of HEK293 cells was correlated with increased caspase 3, depolarization of mitochondrial membrane potential, and DNA fragmentation. The abovementioned finding confirmed that mitochondria play an important role in genotoxicity and cytotoxicity induced by nanoparticles in HEK293 cells. Further, we determined other oxidative stress biomarkers, lipid peroxide (LPO) and glutathione (GSH); LPO was increased and GSH was decreased in HEK293 cells. It is also important to indicate that HEK293 cells appear to be more susceptible to green platinum nanoparticles exposure after 24 hours. This result provides a dose- and time-dependent apoptosis and genotoxicity of green nanoparticles on HEK293 cells.

## Keywords

green platinum nanoparticles, oxidative stress, HEK293 cells, cytotoxicity

## Introduction

The use of nanotechnology in agriculture, the industry that is fast growing, is increasing, and the market size was valued to be more than 1.2 trillion dollars in 2017.<sup>1</sup> Due to its unique characteristic and new features, nanoparticles have been extensively applied in various aspects of daily life and in energy production, catalyst, drugs, cosmetics, and agriculture.<sup>2</sup> The high level of consumption and unrestricted application of nanoparticles have led investigators to study the challenging problems and the impact of their consequences in the environment.<sup>3,4</sup> Due to the rapid evolution and recognition of nanotechnology, the possibility of adverse health effects in animals, humans, and ecosystems has not yet been established. In the present era, bimetallic nanoparticles such iron–platinum are extensively applied in medicines, cancer therapy, bioimaging, drug delivery, hyperthermia, and biosensors.<sup>5</sup> Many investigators have reported that treatment with nanoparticles may affect the

viability of cells and proliferation, and there is very little knowledge about the mechanism of its toxicity.<sup>6</sup> It is supposed that nanoparticles may mess up and damage cellular function through a different mechanism.<sup>7</sup> The nanoparticle has some ions or toxic materials that indirectly or directly affect the living cells via production of reactive oxygen species (ROS). Indeed, it is reported that cell toxicity occurred with the use of xenobiotic

<sup>1</sup> Department of Zoology, College of Science, King Saud University, Riyadh, Saudi Arabia

Received 22 July 2018; received revised 20 September 2018; accepted 25 September 2018

### Corresponding Author:

Saud Alarifi, Department of Zoology, College of Science, King Saud University BOX 2455, Riyadh 11451, Saudi Arabia.  
Email: salarifi@ksu.edu.sa



Creative Commons Non Commercial CC BY-NC: This article is distributed under the terms of the Creative Commons Attribution-NonCommercial 4.0 License (<http://www.creativecommons.org/licenses/by-nc/4.0/>) which permits non-commercial use, reproduction and distribution of the work without further permission provided the original work is attributed as specified on the SAGE and Open Access pages (<https://us.sagepub.com/en-us/nam/open-access-at-sage>).

materials and nanoparticles due to ROS generation.<sup>8,9</sup> Also, an independent component of nanoparticles can induce cellular damage due to its ability to adhere to or to pass through cell membranes.<sup>10</sup> Some researchers have synthesized green nanoparticles using eco-friendly reagents, mostly of biological origin. Mittal et al<sup>11</sup> reported that plants are used in large-scale production of nanoparticles. *Azadirachta indica*, usually known as neem, is a tree in the mahogany Meliaceae family. The leaves of *A indica* are used in synthesizing platinum nanoparticles.

Platinum is one of the rarest and most expensive metals. It has high corrosion resistance and numerous catalytic applications, including automotive catalytic converters and petrochemical cracking catalysts. The platinum drugs, cisplatin, carboplatin, and oxaliplatin, prevail in the treatment of cancer, but new platinum agents have been very slow to enter clinical use.<sup>12</sup> High level of ROS generation induced DNA strand breakage, damaging cellular macromolecules (proteins, fat, and carbohydrate) causing apoptosis.<sup>13</sup>

However, it is not known whether treatment with green platinum nanoparticles may affect the internal organ of an animal or human body systems. Given the delicate structure of the kidney filtration system, along with the major role that this organ plays in the filtration of bodily fluids and the excretion of waste products, it is quite possible that an inappropriate exposure to green platinum nanoparticles may affect renal cell structure and function. To investigate this possibility, the well-characterized human embryonic kidney (HEK293) cell line was chosen as a test system, given the widespread use of these cells to evaluate the cytotoxic effects of chemicals.<sup>14</sup> To determine the effect of green platinum nanoparticles, we treated the HEK293 cells with various dosages to determine the effective acute concentration (EC<sub>50</sub>) for 24 hours. After determining the EC<sub>50</sub> value, we investigated the potential mechanism of cytotoxicity, apoptosis, and genetic damage, using a variety of different approaches. Taken together, our result indicates that treatment using green platinum nanoparticles is correlated with increased cytotoxicity and genotoxicity. Further studies to approve these findings using other types of cells and experimental designs may be warranted.

## Materials and Methods

### Chemicals and Reagents

Green platinum nanoparticles (APS<100 nm particle size) were synthesized by using leaf extract of *Azadirachta indica*. 3-(4,5-dimethylthiazol-2-yl)-5-(3-carboxymethoxyphenyl)-2-(4-sulfophenyl)-2H-tetrazolium (MTS), neutral red dye, 5, 5-dithio-bis-(2-nitrobenzoic acid; DTNB), 2, 7-dichlorofluorescein diacetate, dimethyl sulfoxide, annexin V FITC, and propidium iodide were obtained from Sigma-Aldrich (St. Louis, Missouri, United States). Dulbecco modified Eagle medium (DMEM), fetal bovine serum (FBS), and antibiotics were purchased from Gibco (Ireland). All other chemicals purchased from local suppliers.

### Cell Line and Culture

The HEK293 cells were brought from Research Center King Faisal Specialty Hospital, Riyadh, Saudi Arabia. The HEK293 cells were cultured in DMEM culture medium with FBS (10%) and 100 U/mL antibiotics in a CO<sub>2</sub> (5%) incubator at 37°C. At about 75% confluence, the cells were subcultured into 96-well plates, 6-well plates, and 25-cm<sup>2</sup> flasks according to experimental design.

### Exposure to Green Platinum Nanoparticles

The HEK293 cells were cultured for 18 hours before exposure to green platinum nanoparticles. The stock suspension of platinum nanoparticles was prepared by dissolving at a rate of 1 mg/mL in culture medium and diluted according to the experimental dosages (20-360 µg/mL). The nanoparticle was dispersed in suspension by sonication at 40 KHz for 15 minutes at room temperature prior to treatment. The HEK293 cells were exposed to N-acetyl cysteine (NAC; 5 mmol/L) for 60 minutes prior cotreatment with or without green platinum nanoparticles to confirm the intracellular ROS generation. The control cells were not treated with green platinum nanoparticles.

### Physical Characterization of Green Platinum Nanoparticles

**Transmission Electron Microscopy.** The stock solution of green platinum nanoparticles (1 mg/mL) was prepared in double distilled water. The maximum concentration of green platinum nanoparticles exposure (100 µg/mL) was added on to the carbon-coated copper grid and dried for 24 hours. After drying, the grid image was snapped at 120 kV using transmission electron microscope (TEM; JEOL Inc., Tokyo, Japan). We observed a minimum of 10 sites on the TEM grid.

**Dynamical light scattering.** The size and zeta potential of nanoparticles in aqueous solution were examined using dynamical light scattering (DLS; Nano-Zeta Sizer-HT, Malvern, United Kingdom) as described by Alarifi et al.<sup>15</sup> The green platinum nanoparticle powder was suspended (180 µg/mL) in double distilled water. The suspension was sonicated at 40 W for 10 minutes using a sonicator. The experiment was performed at room temperature.

### Morphological Analysis of Cells

The HEK293 cells were examined for morphological alteration as an effect of treatment with green platinum nanoparticles. The cells were cultured and exposed to various concentrations (0, 20, 60, 180, 360 µg/mL) of green platinum nanoparticles for 6, 24, and 48 hours. The morphology of cells was observed using an inverted phase-contrast microscope (Nikon Eclipse Ti-S; Nikon, Japan).

### MTS Assay for Cell Viability

The toxicity of green platinum nanoparticles on HEK293 cells was examined as described by McGowan et al.<sup>16</sup> Briefly,  $1 \times 10^4$  cells per well were cultured in culture plate (96 well) and treated with various doses (0, 20, 60, 180, and 360  $\mu\text{g}/\text{mL}$ ) of green platinum nanoparticles for 6, 24, and 48 hours. After exposure, the culture media were removed from 96-well plates and 100  $\mu\text{L}$  MTS (Promega Corp, Madison, Wisconsin) was added. The reagent was added directly to the wells, and cells incubated at  $37^\circ\text{C}$  for a minimum of 2 hours. Assessment of metabolic activity was recorded as relative colorimetric changes measured at 492 nm using a microplate reader (Synergy-HT; BioTek, Winooski, Vermont).

### NRU Assay

Different concentrations of green platinum nanoparticle (0, 20, 60, 180, 360  $\mu\text{g}/\text{mL}$ ) were exposed to HEK293 cells for 6, 24, and 48 hours. After treatment with nanoparticles, the cells were rinsed with chilled phosphate-buffered saline (PBS). The cell culture plates were incubated for 4 hours with NR dye (50  $\mu\text{g}/\text{mL}$ ) containing DMEM. The optical density was measured at 540 nm.<sup>17</sup>

### Reactive Oxygen Species

The HEK293 cells ( $2 \times 10^4$  cells/well) were cultured in black 96-well plates for 24 hours and exposed to green platinum nanoparticles (0, 20, 60, 180, and 360  $\mu\text{g}/\text{mL}$ ) for 6, 24, and 48 hours. After exposure, the HEK293 cells were incubated with H2DCF-DA for 35 minutes. After incubation, the fluorescence of DCF was determined using microplate spectrofluorometer (Spectra MAX Gemini EM; Molecular Devices) applying excitation wavelength of 480 nm and emission wavelength of 530 nm. Generation of ROS was further confirmed by treatment with NAC (5 mmol/L) as a scavenger.<sup>18</sup>

As a parallel experiment, cells ( $1 \times 10^3$  cells/well) in a 6-well transparent plate were examined for intracellular ROS generation using a fluorescent microscope (Olympus CKX41; Olympus, Center Valley, Pennsylvania), with images taken at  $10\times$  magnification.

### Cell Lysate

The cell lysates were prepared from control and nanoparticle-treated HEK293 cells for observation of reduced glutathione (GSH) and lipid peroxide (LPO). Concisely, HEK293 cells were cultured in  $25\text{-cm}^2$  flask and treated with green platinum nanoparticles (0, 20, 60, 180, and 360  $\mu\text{g}/\text{mL}$ ) for 24 and 48 hours. The treated cells were washed with chilled PBS and scrapped. The scrapped cells were lysed in cell lysis buffer (1  $\times$  20 mmol/L Tris-HCl, pH 7.5, 150 mmol/L NaCl, 1 mmol/L  $\text{Na}_2\text{EDTA}$ , 1% Triton, and 2.5 mmol/L sodium pyrophosphate). After centrifugation (15 000g for 10 minutes at  $4^\circ\text{C}$ ), the supernatant (cell lysate) was incubated on ice for further tests. The amount of protein in the cell lysate was

determined by Bradford method<sup>19</sup> using bovine serum albumin as the standard.

**Glutathione Assay.** The level of GSH was measured using Ellman method.<sup>20</sup> The cell lysate (100  $\mu\text{L}$ ) was mixed with 900  $\mu\text{L}$  TCA (5%) and centrifuged at 3000 g for 10 minutes at  $4^\circ\text{C}$ . The supernatant (500  $\mu\text{L}$ ) was mixed with DTNB (0.01%, 1.5 mL), and optical density of the mixture was observed at 412 nm. The quantity of glutathione was represented in (%) percentage when compared to the control.

**Lipid peroxide test.** Lipid peroxide level was determined by measuring the formation of malondialdehyde (MDA) using the method of Ohkawa et al.<sup>21</sup> The cell lysate (100  $\mu\text{L}$ ) was mixed with 1.9 mL sodium phosphate buffer (0.1 mol/L, pH 7.4) and incubated for 60 minutes at  $37^\circ\text{C}$ . After incubation, 5% **trichloroacetic acid** was added and centrifuged at 3000g for 10 minutes at room temperature to obtain a supernatant. The supernatant was mixed with 1 mL tert-Butyl alcohol (1%) and put in a water bath at  $100^\circ\text{C}$  for 30 minutes. The optical density of the cooled mixture was examined at 532 nm and was converted to MDA and expressed in terms of percentage when compared to the control.

### Rhodamine 123 Staining for Mitochondrial Membrane Potential

Mitochondrial membrane potential (MMP) was visualized using Rhodamine 123 fluorescent stain. The HEK293 cells were treated with green platinum nanoparticles (20, 60, 180, and 360  $\mu\text{g}/\text{mL}$ ) for 24 and 48 hours. After treatment, the cells were incubated with Rhodamine 123 (20  $\mu\text{mol}/\text{L}$ ; Cayman chemical) for 40 minutes at  $37^\circ\text{C}$ , rinsed, and images were obtained by fluorescence microscope, and fluorescent intensity of control and treated cells were read by using the microplate reader.<sup>22</sup>

### Damage of Lysosome

The damaged and healthy cell lysosome were traced using acridine orange (AO) shifting method. The cells were treated with green platinum nanoparticles (180 and 360  $\mu\text{g}/\text{mL}$ ) for 24 and 48 hours. Next, the exposed cells were rinsed with ice-cold PBS and stained with AO (10  $\mu\text{g}/\text{mL}$ ) for 20 minutes at room temperature. The image of all exposure concentration and control cells was taken using fluorescence microscope with green and red filters.

### Assessment of Chromosome Condensation and Caspase 3 Activity

The mutagenic effect of green platinum nanoparticles on HEK293 was examined using DAPI staining. The condensed chromatin body in exposed cells was observed according to Toné et al method.<sup>23</sup> The activity of caspase-3 enzyme was

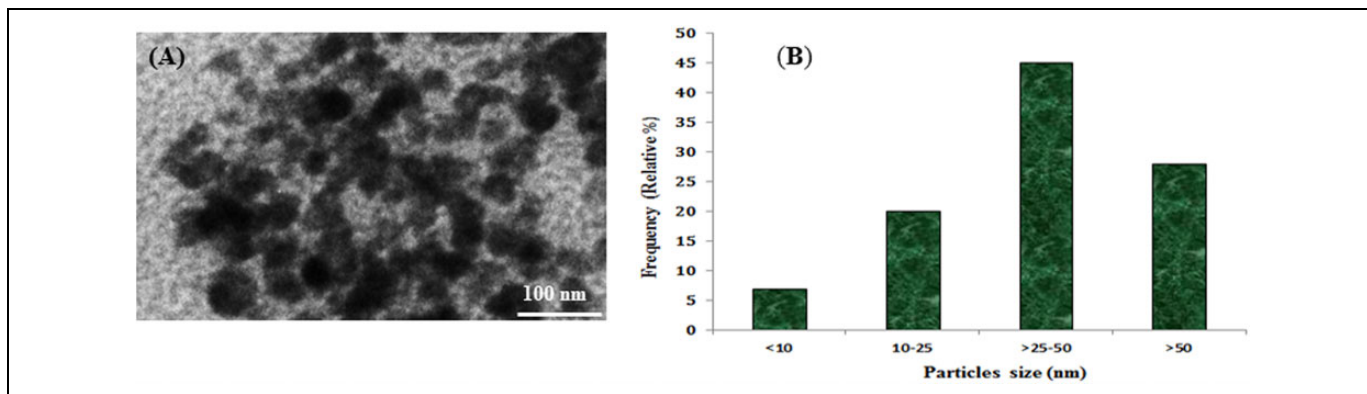


**Figure 1.** A, Transmission electron microscope (TEM) image of green platinum nanoparticles B, Frequency and (%) of green platinum nanoparticles by size distinction.

examined in HEK293 cells using Cayman Chemical colorimetric assay kits.

### Quantitative Real-Time Polymerase Chain Reaction Analysis

The HEK 293 cells were grown in 6-well plates and exposed to green platinum nanoparticles (180  $\mu\text{g}/\text{mL}$ ) for 48 hours. Total RNA was isolated from untreated and treated cells by Qiagen RNeasy Mini Kit (Valencia, California) according to the manufacturer's instruction. The quantity of RNA was measured using a Nanodrop 8000 spectrophotometer (Thermo-Scientific, Wilmington, Delaware).

Complementary DNA (cDNA) was synthesized from RNA by the reverse transcription and used M-MLV (Promega, Madison, Wisconsin) and oligo (dT) primers (Promega) as described in manufacturer's instructions.

Real-time polymerase chain reaction (RT-PCR) was used by applying the Quanti Tect SYBR Green PCR kit (Qiagen) using the ABI PRISM 7900HT Sequence Detection System (Applied Biosystems, Foster City, California). The template cDNA (2  $\mu\text{L}$ ) was mixed with reaction mixture (20  $\mu\text{L}$ ). The RT-PCR cycle parameters were: 10 minutes at 95°C followed by 40 cycles involving denaturation at 95°C for 15 seconds, annealing at 60°C for 20 seconds, and elongation at 72°C for 20 seconds.

The PCR analysis was done using primer sequences of apoptotic genes such as bax and bcl2, and  $\beta$  actin expression was used as a control. Gene-specific primer sequences are as follows:

$\beta$ -Actin -F-CCAACCGCGAGAAGATGA, R-CCAGAGGCGTACAGGGATAG  
 Bax -F-TTCATCCAGGATCGAGCAGG, R-TGAGACACTCGCTCAGCTTC  
 Bcl2-F-TGGACAACCATGACCTTGGACAATCA, R- TCCATCCTCCACCAGTGTTCCCATC

The selected gene expression was normalized to the  $\beta$ -actin gene, which was used as an internal housekeeping control.

### Alkaline Single-Cell Gel Electrophoresis

Comet assay was used to examine the DNA damaging potential of green platinum nanoparticles on HEK293 cells according to Ali et al's method.<sup>24</sup> HEK293 cells (50 000 cells per well) was cultured in 6-well plates and exposed to different concentrations of green platinum nanoparticles for 24 and 48 hours. On completing the exposure of nanoparticles, the cells were trypsinized and centrifuged at 1200 rpm for 5 minutes and suspended in cold culture medium. Twenty thousand cells (15  $\mu\text{L}$ ) were mixed with low melting point agarose (85  $\mu\text{L}$ , 0.5%) and embedded on the pre-coated agarose slide. After solidification of the slide, it was immersed in lysis buffer for 24 hours; the next day it was immersed in alkaline electrophoresis buffer for 20 minutes for DNA strand unwinding and electrophoresis was done at 300 mA, 16 mV for 30 minutes. After electrophoresis, the slide was washed using neutralizing solution and stained with ethidium bromide. The cell image of 50 random cells (25 from each replicate slide) was analyzed for each experiment. Single-strand breakage was determined as % tail DNA and olive tail moment using Kamet software 5.1.

### Statistical Analysis

The significant value of the present data was analyzed by using 1-way analysis of variance, and the significant and highly significant value were fixed at  $P < .05$  and  $P < .01$ , respectively. Data were expressed as the average value of triplicate in independent experiment.

## Results

### Green Platinum Nanoparticles

The nature, size, and shape of green platinum nanoparticles were examined by TEM and DLS methods. We counted the mean diameter of 50 green platinum nanoparticles on a copper grid, and its average size was  $24.6 \pm 3.4$  nm. Figure 1A shows the TEM image of green platinum nanoparticles. The frequency (%) of size scattering of green

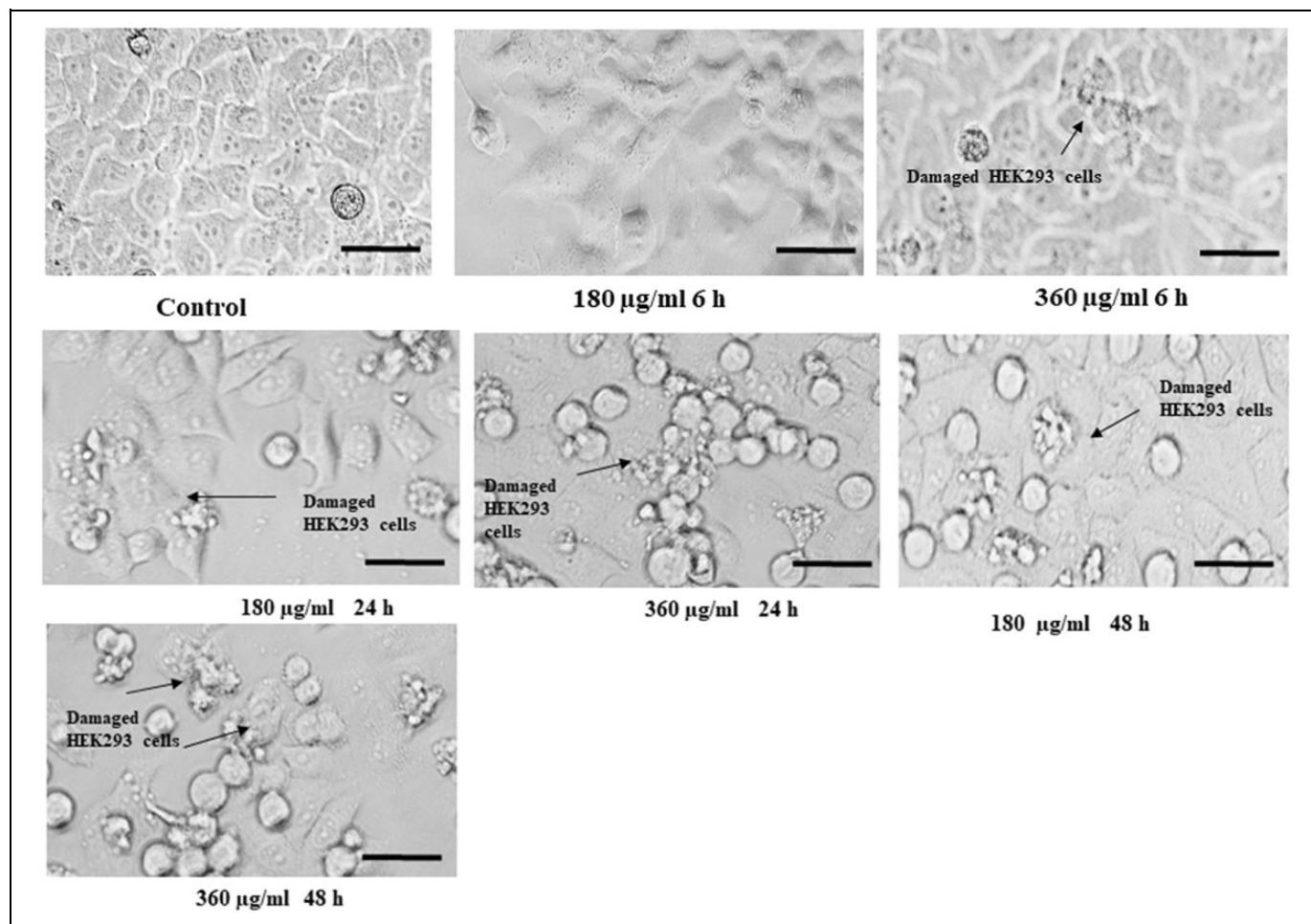


**Figure 2.** Morphological changes in HEK293 cells exposed to different concentrations of green platinum nanoparticles for 6, 24, and 48 hours. Scale bar is 50  $\mu\text{m}$ .

platinum nanoparticles is shown in Figure 1B. The aqueous size of green platinum nanoparticles in distilled water was  $160 \pm 10$  nm. The zeta-potential of green platinum nanoparticles in water was  $-11$  mV.

### Morphology of HEK293 Cells

After exposure of green platinum nanoparticles, the shape of HEK293 cell was altered into round shape and detached from the surface of the flask at higher concentration (180 and 360  $\mu\text{g}/\text{mL}$ ; Figure 2). We noticed that there are no changes in lower concentration.

**Cytotoxicity.** HEK293 cells were treated with different concentrations (20–360  $\mu\text{g}/\text{mL}$ ) of green platinum nanoparticles for 6, 24, and 48 hours, and cell viability was determined by the MTS and NRU tests. Results of MTS assay indicated that cell viability was found to 99.06%, 96.9%, 98.5% and 88.5% for 6 hours; 95%, 91%, 83.9%, and 70.5% for 24 hours; and 90%, 86%, 68.25%, and 54.15% for 48 hours (Figure 3A). Green platinum nanoparticles induced cytotoxicity in a concentration- and time-dependent manner. The results of the NRU assay

were in accordance with the MTS assay (Figure 3B). The correlation of cytotoxicity of green platinum nanoparticles with MTS and NRU assays is shown in Figure 3C.

**Oxidative Stress.** Generation of ROS in HEK293 cells after exposure to green platinum nanoparticles was increased in a concentration- and time-dependent manner (Figure 4A and B). Maximum ROS generation was observed at 360  $\mu\text{g}/\text{mL}$ , and it was increased by 122% compared to control for 48 hours. Fluorescent microscopy result showed that the HEK293 cells exposed to green platinum nanoparticles (360  $\mu\text{g}/\text{mL}$ ) expressed high intensity of green fluorescent DCF (an indicator of ROS generation) in comparison to control (Figure 4A). The production of ROS in HEK293 cells treated with green platinum nanoparticles at 360  $\mu\text{g}/\text{mL}$  was 13%, 50%, and 48% in the presence of NAC (5 mmol/L) for 6-, 24-, and 48-hour exposure periods, respectively (Figure 4A and B).

Ayala et al<sup>25</sup> reported that high quantity of free radicals or ROS can inflict direct damage to lipids. The MDA quantity, which is an end product of lipid peroxide, was increased significantly, and the level of GSH was declined in a

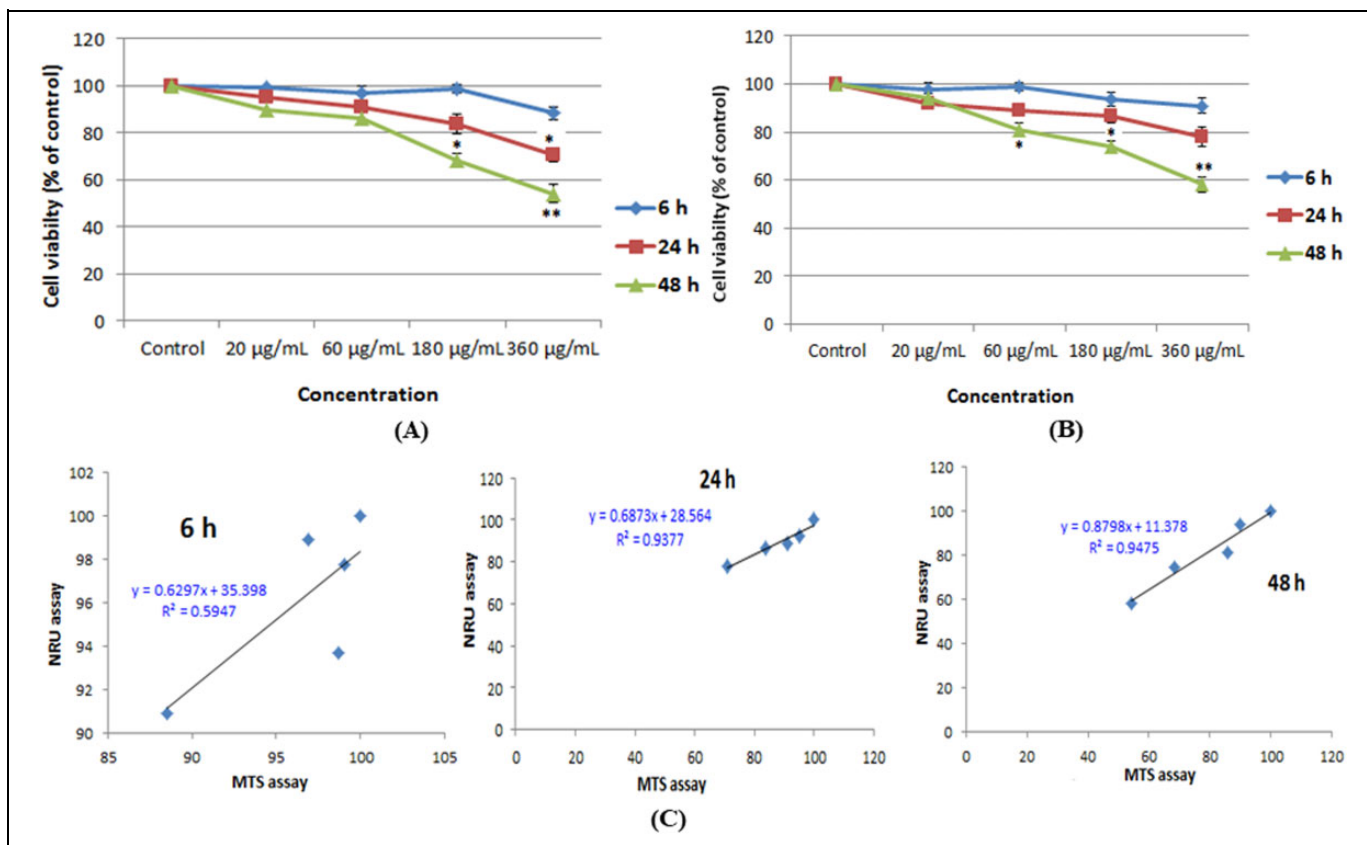


**Figure 3.** Cytotoxicity of green platinum nanoparticles in HEK293 cells for 4, 24, and 48 hours. As determined by (A) MTS and (B) NRU. Each value represents the mean (SE) of 3 experiments.  $n = 3$ ,  $*P < .05$  and  $**P < .01$  versus control. (C) Correlation of MTS and NRU assays cell percentage viability of HEK293 cells.

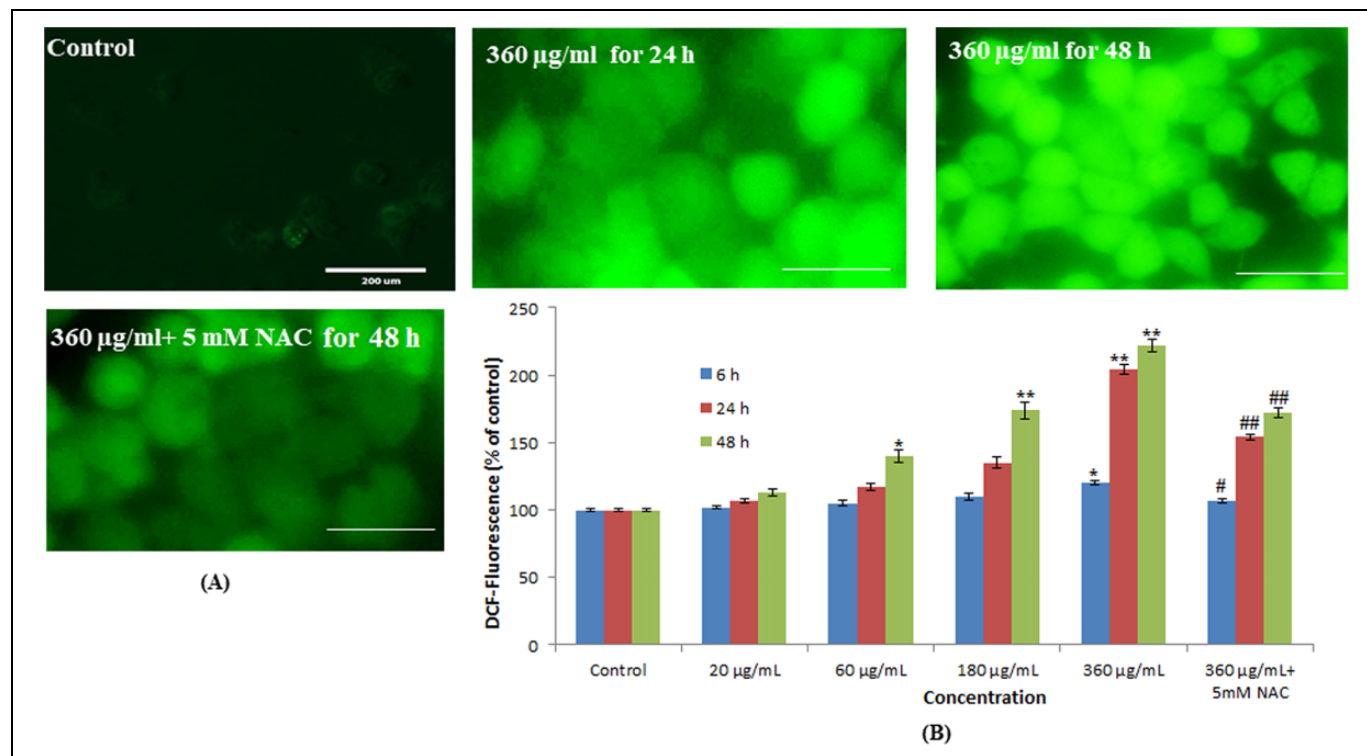


**Figure 4.** Generation of reaction oxygen species (ROS) in HEK293 cells due to green platinum nanoparticles. A, The fluorescence image of HEK293 cells treated with 360 µg/mL of nanoparticles for 24 h and 48 h and stained with DCFKIM. (B) ROS production due to green platinum nanoparticles in HEK293 cells. Each value represents the mean (SE) of 3 experiments.  $*P < .05$  and  $**P < 0.01$  versus control.  $\#P < .05$  and  $\#\#P < .01$  versus HEK 293 cells treated with 360 µg/mL of nanoparticles.

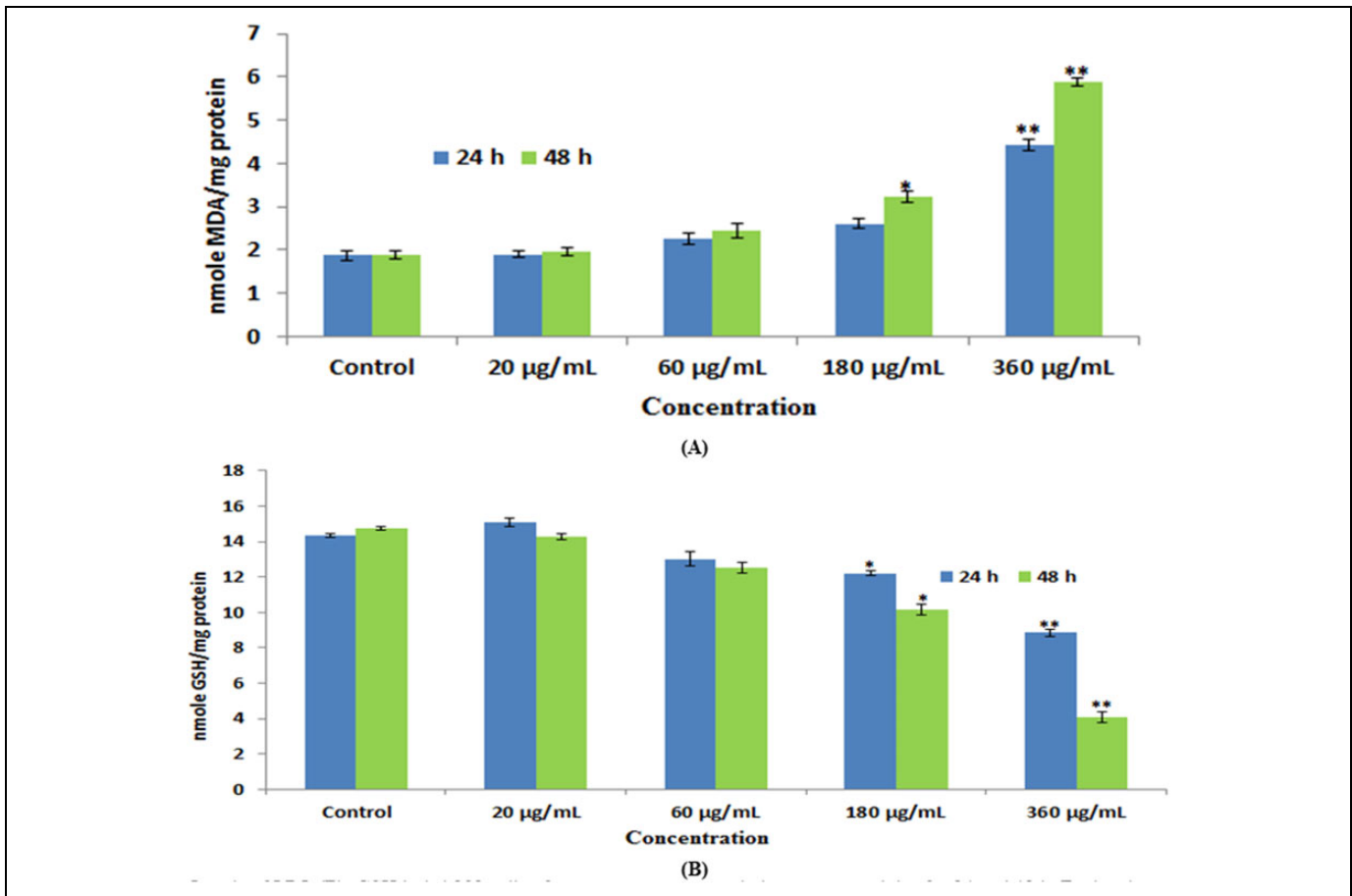


**Figure 5.** A, Levels of lipid peroxide (LPO). B, Glutathione (GSH) in HEK293 cells after exposure to green platinum nanoparticles for 24 and 48 hours. Each value represents the mean (LSE) of 3 experiments, \*P < .05 and \*\*P < .01 versus control.

concentration- and time-dependent manner in cells treated with green platinum nanoparticles (Figure 5A and B).

**Mitochondrial membrane potential and damage of lysosome membrane.** Mitochondrial membrane potential was assessed by a Rhodamine 123 staining method based on the principle of development of fluorescent intensity. Some researchers reported that MMP declined in apoptotic and necrotic cells.<sup>26</sup> Untreated cells expressed deep red fluorescence which indicates normal MMP (Figure 6A and B). The cells treated with 180 and 360 µg/mL of green platinum nanoparticles had declined MMP, and decline in red fluorescence indicates loss of MMP (Figure 6 C-F).

The effect of green platinum nanoparticles on cell organelle lysosome was observed using AO dye, and it exhibited red fluorescence to the healthy lysosome (highly acidic pH) as observed in control. Green platinum nanoparticle-exposed HEK293 cells produced fragmentation of lysosome membrane (lower acidic pH). As a consequence, the AO dye leaked out in the cytoplasm, red fluorescence merged with green fluorescence, and formed an orange fluorescence, which is a characteristic of damaged lysosome (Figure 6 G-I). Thus, these findings indicate decline in MMP and lysosome in HEK293

cells due to treatment with green platinum nanoparticles, and as a consequence cytotoxicity occurred in HEK293 cells.

**Apoptosis.** The untreated cells showed intact nucleus with blue fluorescence, but apoptotic cells have fragmented chromatin with high blue intensity. Green platinum treatment induced maximum apoptotic cells when compared to control (Figure 7A).

Caspase 3 enzymes are hallmark of apoptosis, and it was significantly increased in green platinum nanoparticles-treated cells. The activity of the caspase-3 enzyme has significantly increased in a dose- and time-dependent manner (Figure 7B).

Further, we examined the expression of apoptotic genes Bax and Bcl2 (Figure 8). The expressed apoptotic gene Bax was upregulated (Figure 8A) and Bcl2 was downregulated (Figure 8B). Our finding indicate that Bcl2 gene plays an important role in apoptosis of HEK293 cells.

**DNA damage.** The genotoxic potential of green platinum nanoparticles in HEK293 cells was examined by comet assay. The cells treated with various concentrations of nanoparticles expressed significant DNA damage compared to untreated cells (Figure 9 A-D). In nanoparticles-treated cells, the percentage of tail DNA was 36% compared to control (4.6%). Also, the

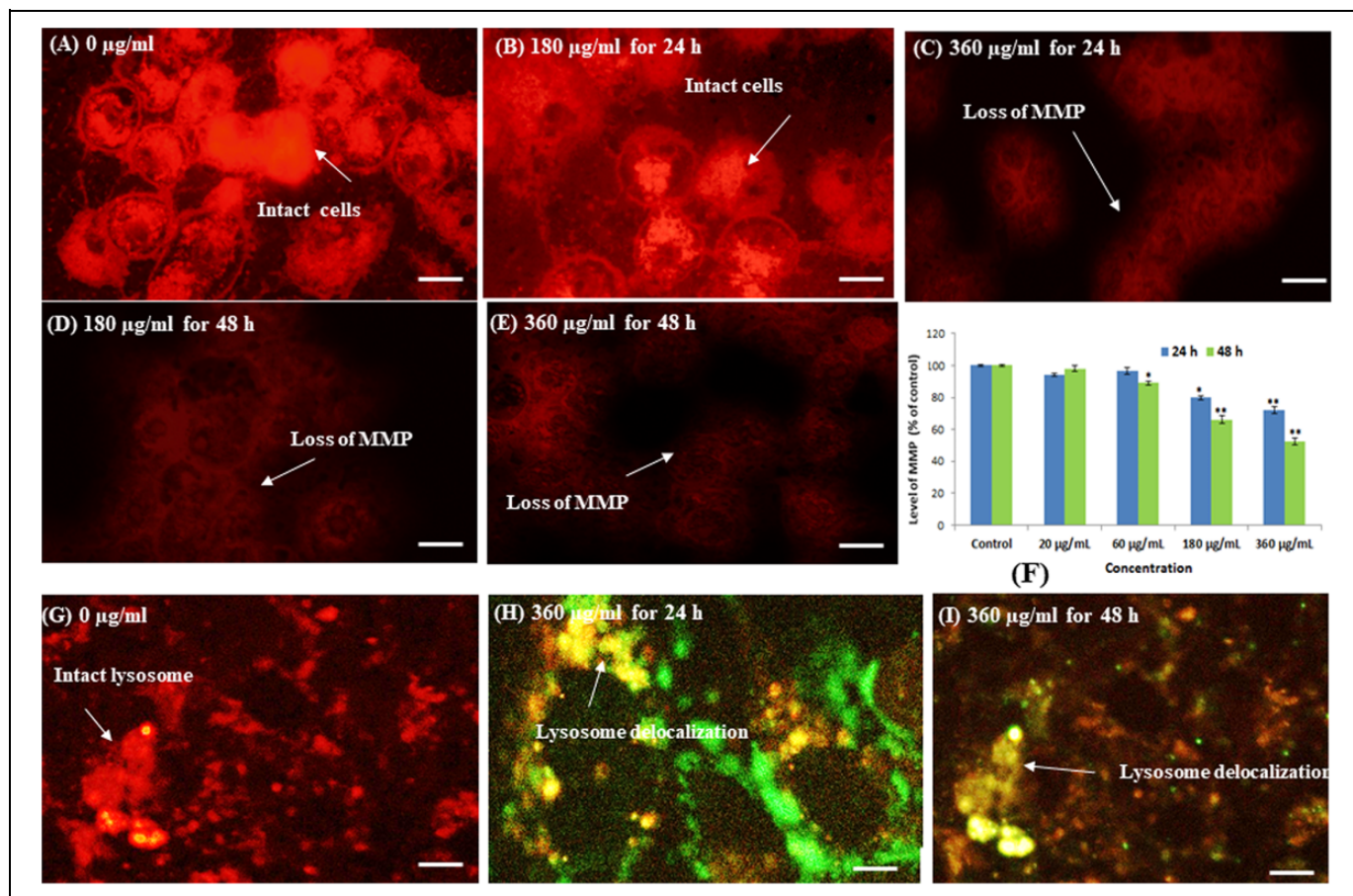


**Figure 6.** Images representing MMP loss (A-E) and lysosome delocalization (G-I) in HEK293 cells after green platinum nanoparticle exposure at concentrations of 180 and 360 µg/mL for 24 and 48 hours. (A) Control cells. (B) 180 µg/mL for 24 hours. (C) 360 µg/mL for 24 hours. (D) 180 µg/mL for 48 hours. (E) 360 µg/mL for 48 hours. (F) Percentage of loss of 501P in HEK293 cells. The lysosome delocalization in HEK293 cells (G). Control cells (H). 360 µg/mL for 24 hours (I). 360 µg/mL for 48 hours. Each value represents the mean (SE) of 3 experiments. \* $P < .05$  and \*\* $P < .01$  vs control.

maximum olive tail moment (8.05 AU) was observed in nanoparticle-treated cells compared to control (0.34 AU).

## Discussion

The fast progress in nanotechnology and the possible discharge of nanoparticles and their ions into the environment have drawn considerable attention. Herbal plants are an important part of the ecosystem, and the correlation between nanoparticles and plants is the obligatory part of the risk assessment. Nowadays nanomaterials are applied in the industry due to their unique physicochemical properties. Platinum nanoparticles are used in drugs, for example, cisplatin. Bendale et al<sup>27</sup> have reported that cisplatin was restricted as it induces nephrotoxicity, neurotoxicity, ototoxicity, and myelosuppression and due to the intrinsic and acquired resistance developed by various cancers. The design of nanoparticles size, shape, and surface chemistry has a significant effect on their functions. The size and shape are the basic properties of the nanoparticles which are important for their biological activities. Most nanoparticles are sphere-shaped. Before the exposure to green

platinum nanoparticles, we characterized the shape through TEM and DLS. The size of nanoparticles was bigger when observed through DLS compared to TEM. The difference is attributed to solvent. Nanoparticles cause harmful effect due to surface chemistry, size, and shape.<sup>28</sup>

In this study, we determined the cytotoxic potential of green platinum nanoparticle on HEK293 using MTS and NRU assays. Lobo et al<sup>29</sup> have reported that more active hydroxyl radical outbreak in components of cells, for example, lipid, proteins, DNA, induced the oxidative effect. In this experiment, green platinum nanoparticles increased DNA tail length and olive tail moment in single-cell gel electrophoresis, which determines DNA strand breakage as alkali labile site.<sup>30</sup> Formation of MDA as a product of LPO in HEK293 cells due to green platinum nanoparticles treatment was observed by LPO assay. On the other hand, excess ROS generation was due to the green platinum nanoparticle, and as a consequence oxidative damage and apoptosis occurred.<sup>31</sup> Generation of ROS, decline in GSH and LPO, and DNA damage are due to the green platinum nanoparticle in cells, leading to damage of cellular component. Mohammadi et al<sup>32</sup> reported that

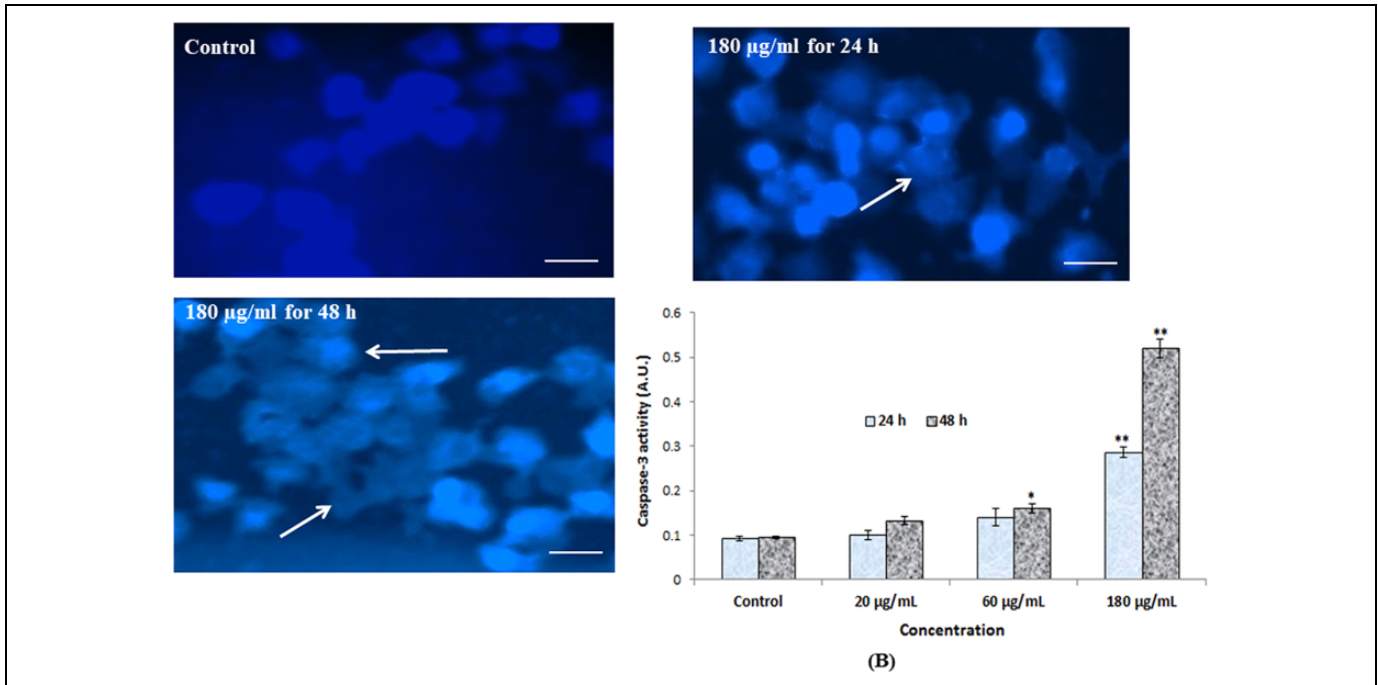


**Figure 7.** (A) Chromosomal condensation and (B) induction of caspase-3 in HEK293 cells after exposure to green platinum nanoparticle for 24 and 48 hours. Each value represents the mean (SE) of 3 experiments. \* $P < .05$  and \*\* $P < .01$  versus control. Arrow indicates fragmented chromosome.

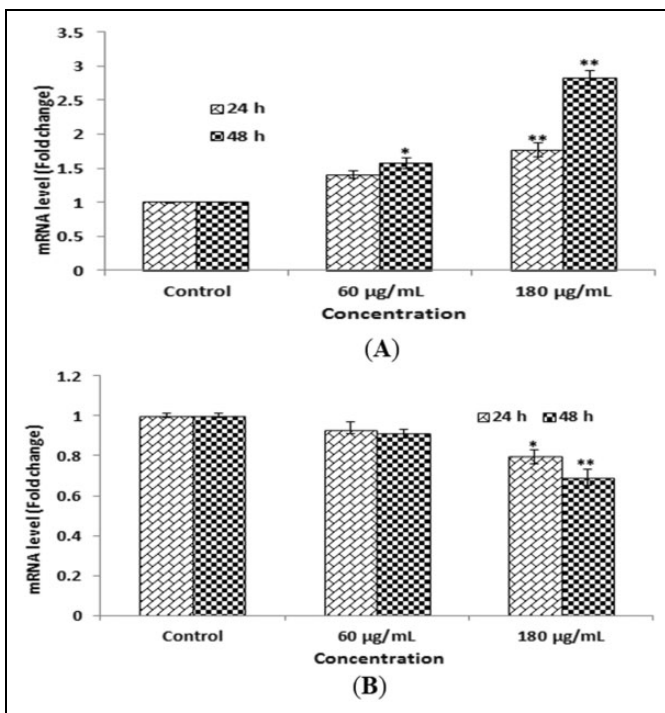


**Figure 8.** Quantitative real-time polymerase chain reaction (PCR) analysis of messenger RNA (mRNA) levels of apoptotic genes in HEK293 cells exposed green platinum nanoparticles for 24 and 48 hours. The expression of (A) Bax and (B) Bcl2. Results are expressed average  $\times$  SE of triplicate experiments.

platinum nanoparticles induced cytotoxicity and apoptosis via generation of ROS in MCF-7 and HepG2 cells. But the role of ROS generation in green platinum nanoparticle-induced cytotoxicity in HEK293 cells is unclear. The generation of ROS occurred in a concentration and time-dependent manner as presented in Figure 4 and may be the reason for cell death. To determine the probable cause of nanoparticle-induced cell death, we examined the alteration in different biomarkers involved in apoptosis.

Susin et al<sup>33</sup> suggested that mitochondria play an important role in apoptosis, and compromise of mitochondrial integrity may be prevented by various biomarkers of apoptosis. Oxidative stress leads to activation of caspase enzymes via involvement of cytochrome C in the intermembrane space into the cytoplasm.<sup>34</sup> In the present study green platinum nanoparticles induced loss of MMP. Finucane et al<sup>35</sup> have reported that bcl-2 inhibits the opening of mitochondrial membrane pores, while Bax leads to the opening of membrane pores during apoptosis. In this study, we found compromise in MMP due to green platinum nanoparticles as a consequence of upregulation of Bax and downregulation of bcl2. Our results show caspase-3 activity was increased in a time- and dose-dependent manner. Marullo et al<sup>36</sup> have reported that mitochondria are important cell organelles for cisplatin production and ROS generation. This put forward that platinum initiates the intrinsic pathway of apoptosis, which is mediated by the up- and downregulation of Bax and bcl2 expression from mitochondria.

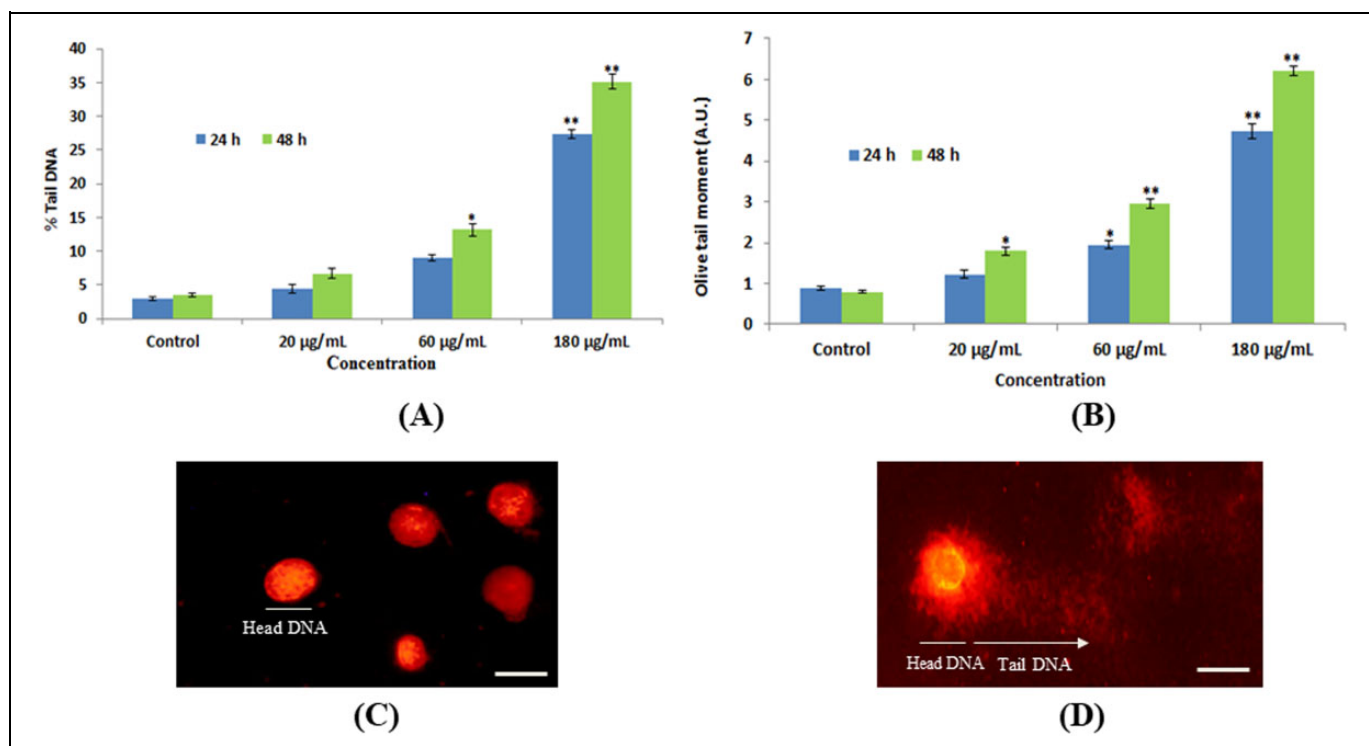


**Figure 9.** DNA damage in HEK293 cells due to green platinum nanoparticles. (A) Tail DNA (%) (B) Olive tail moment. (C) Control cell. (D) Treated cell (180 µg/mL of green platinum nanoparticle). Each value represents the mean (SE) of 3 experiments. \* $P < .05$  and \*\* $P < .01$  versus control. Scale bar is 50 µm.

In conclusion, green platinum nanoparticles induced oxidative stress, and reducing the level of GSH lead to damage of the cell components of HEK293 cells. Green platinum nanoparticles compromise apoptosis via mitochondrial- and caspase-3-dependent manner in HEK293 cells.

### Declaration of Conflicting Interests

The author(s) declared no potential conflicts of interest with respect to the research, authorship, and/or publication of this article.

### Funding

The author(s) disclosed receipt of the following financial support for the research, authorship, and/or publication of this article: The authors would like to extend their sincere appreciation to the Deanship of Scientific Research at King Saud University for its funding of this research through the research Group Project No. RGP-180.

### ORCID iD

Saad Alkahtani  <https://orcid.org/0000-0003-4613-3776>

### References

- Industry ARC. Nano fertilizers industry 2017 global market growth, trends, share, size and 2022 forecast report. [https://www.sharewise.com/us/news\\_articles/Nano\\_Fertilizers\\_Industry\\_2017](https://www.sharewise.com/us/news_articles/Nano_Fertilizers_Industry_2017) (accessed 17 November 2017).
- Nel A, Xia T, Madler L, Li N. Toxic potential of materials at the nano level. *Science*. 2006;311(5761):622-627.
- Gottschalk F, Lassen C, Kjoelhol J, Christensen F, Nowack B. Modeling flows and concentrations of nine engineered nanomaterials in the Danish environment. *Int J Environ Res Public Health*. 2015;12(5):5581-5602.
- Tolaymat T, El Badawy A, Sequeira R, Genaidy A. A system-of-systems approach as a broad and integrated paradigm for sustainable engineered nanomaterials. *Sci Total Environ*. 2015;511:595-607.
- McNamara K, Tofail SAM. Nanoparticles in biomedical applications. *Adv Phy: X*. 2017;2(1):54-88.
- AshaRani PV, Low Kah Mun G, Hande MP, Valiyaveettil S. Cytotoxicity and genotoxicity of silver nanoparticles in human cells. *ACS Nano*. 2009;3(2):279-290.
- Huang YW, Cambre M, Lee HJ. The toxicity of nanoparticles depends on multiple molecular and physicochemical mechanisms. *Int J Mol Sci*. 2017;18(12):E2702.
- Markovic Z, Trajkovic V. Biomedical potential of the reactive oxygen species generation and quenching by fullerenes (C60). *Biomaterials*. 2008;29(26):3561-3573.
- Alarifi S, Ali D, Alkahtani S, Almeer RS. ROS-mediated apoptosis and genotoxicity induced by palladium nanoparticles in human skin malignant melanoma cells. *Oxid Med Cell Longev*. 2017;2017:10. Article ID 8439098.
- Verma A, Uzun O, Hu Y, et al. Surface-structure-regulated cell-membrane penetration by monolayer-protected nanoparticles. *Nat Mater*. 2008;7(7):588-595.
- Mittal AK, Chisti Y, Banerjee UC. Synthesis of metallic nanoparticles using plant extracts. *Biotechnol Adv*. 2013;31(2):346-356.

12. Johnstone TC, Suntharalingam K, Lippard SJ. The next generation of platinum drugs: targeted Pt(II) agents, nanoparticle delivery, and Pt (IV) prodrugs. *Chem Rev.* 2016;116(5):3436-3486.
13. Sadeghnia HR, Jamshidi R, Afshari AR, Mollazadeh H, Forouzanfar F, Rakhshandeh H. Terminalia chebula attenuates quinolinate-induced oxidative PC12 and OLN-93 cell death. *Mult Scler Relat Disord.* 2017;14:60-67.
14. Chou CC, Riviere JE, Monteiro-Riviere NA. The cytotoxicity of jet fuel aromatic hydrocarbons and dose-related interleukin-8 release from human epidermal keratinocytes. *Arch Toxicol.* 2003;77(7):384-391.
15. Alarifi S, Ali D, Alkahtani S. Nanoalumina induces apoptosis by impairing antioxidant enzyme systems in human hepatocarcinoma cells. *Intern J Nanomed.* 2015;10(1):3751-3760.
16. McGowan EM, Alling N, Jackson EA, et al. Evaluation of cell cycle arrest in estrogen responsive MCF-7 breast cancer cells: pitfalls of the MTS assay. *PLoS One.* 2011;6(6):e20623.
17. Borenfreund E, Puerner JA. Toxicity determination in vitro by morphological alterations and neutral red absorption. *Toxicol. Lett.* 1985;24(2-3):119-124.
18. Halasi M, Wang M, Chavan TS, Gaponenko V, Hay N, Gartel AL. ROS inhibitor N-acetyl-l-cysteine antagonizes the activity of proteasome inhibitors. *Biochem J.* 2013;454(2):201-208.
19. Bradford MM. A rapid and sensitive method for the quantitation of microgram quantities of protein utilizing the principle of protein-dye binding. *Anal. Biochem.* 1976;72(1-2):248-254.
20. Ellman GL. Tissue sulfhydryl groups. *Arch. Biochem. Biophys.* 1959;82(1):70-77.
21. Ohkawa H, Onishi N, Yagi K. Assay for lipid peroxidation in animal tissue by thiobarbituric acid reaction. *Anal. Biochem.* 1979;95(2):351-358.
22. Alkahtane AA, Alarifi S, Al-Qahtani AA, et al. Cytotoxicity and genotoxicity of cypermethrin in hepatocarcinoma cells: a dose- and time-dependent study. *Dose Response.* 2018;16(2):1-9.
23. Tone S, Sugimoto K, Tanda K, et al. Three distinct stages of apoptotic nuclear condensation revealed by time-lapse imaging, biochemical and electron microscopy analysis of cell-free apoptosis. *Exp Cell Res.* 2007;313(16):3635-3644.
24. Ali D, Nagpure NS, Kumar S, Kumar R, Kushwaha B. Genotoxicity assessment of acute exposure of chlorpyrifos to freshwater fish channa punctatus (Bloch) using micronucleus assay and alkaline single-cell gel electrophoresis. *Chemosphere* 2008;71(10):1823-1831.
25. Ayala A, Munoz MF, Arguelles S. Lipid peroxidation: production, metabolism, and signaling mechanisms of malondialdehyde and 4-hydroxy-2-nonenal. *Oxid Med Cel Long.* 2014;2014:31. Article ID 360438
26. Webster KA. Mitochondrial membrane permeabilization and cell death during myocardial infarction: roles of calcium and reactive oxygen species. *Future Cardiol.* 2012;8(6):863-884.
27. Bendale Y, Bendale V, Paul S. Evaluation of cytotoxic activity of platinum nanoparticles against normal and cancer cells and its anticancer potential through induction of apoptosis. *Integr Med Res.* 2017;6(2):141-148.
28. Sharma D, Kanchi S, Bisetty K. Biogenic synthesis of nanoparticles. A review. *Arabian J Chem.* 2015. <http://dx.doi.org/10.1016/j.arabjc.2015.11.002>
29. Lobo V, Patil A, Phatak A, Chandra N. Free radicals, antioxidants and functional foods: impact on human health. *Pharmacogn Rev.* 2010;4(8):118-126.
30. Mozaffarieh M, Schoetzau A, Sauter M, et al. Comet assay analysis of single-stranded DNA breaks in circulating leukocytes of glaucoma patients. *Mol Vis.* 2008;14:1584-1588.
31. Dayem AA, Hossain MK, Lee SB, et al. The role of reactive oxygen species (ROS) in the biological activities of metallic nanoparticles. *Int J Mol Sci.* 2017;18(1):E120.
32. Mohammadi H, Abedi A, Akbarzade A, et al. Evaluation of synthesized platinum nanoparticles on the MCF-7 and HepG-2 cancer cell lines. *Int Nano Lett.* 2013;3:28.
33. Susin SA, Zamzami N, Kroemer G. Mitochondria as regulators of apoptosis: doubt no more. *Biochim Biophys Acta.* 1998;1366(1-2):151-165.
34. Yuan J, Murrell GA, Trickett A, Wang MX. Involvement of cytochrome c release and caspase-3 activation in the oxidative stress-induced apoptosis in human tendon fibroblasts. *Biochimica et Biophysica Acta - Mol Cell Res.* 2003;1641(1):35-41.
35. Finucane DM, Wetzel EB, Waterhouse NJ, Cotter TG, Green DR. Bax-induced caspase activation and apoptosis via cytochrome release from Mitochondria is inhibitable by Bcl-xL. *J Bio. Chem.* 1999;274(4):2225-2233.
36. Marullo R, Werner E, Degtyareva N, et al. Cisplatin induces a mitochondrial-ROS response that contributes to cytotoxicity depending on mitochondrial redox status and bioenergetic functions. *PLoS One.* 2013;8(11):e81162.